J. Membrane Biol. 176, 119–131 (2000)
DOI: 10.1007/s00232001078

The Journal of
Membrane
Biology

Analysis of the Structure and Electrophysiological Actions of Halitoxins: 1,3 Alkyl-pyridinium Salts from *Callyspongia ridleyi*

R.H. Scott[1], A.D. Whyment[1], A. Foster[1], K.H. Gordon[2]*, B.F. Milne[2], M. Jaspars[2]
[1]Department of Biomedical Sciences, Institute of Medical Sciences, Aberdeen University, Foresterhill, Aberdeen AB25 2ZD, UK
[2]Marine Natural Products Laboratory, Department of Chemistry, University of Aberdeen, Old Aberdeen, AB24 3UE, UK

Received: 23 December 1999/Revised: 3 April 2000

Abstract. We have chemically characterized a preparation of halitoxins, (1,3 alkyl-pyridinium salts) isolated from the marine sponge *Callyspongia ridleyi*. At concentrations of 50 and 5 μg/ml the halitoxin preparation caused irreversible membrane potential depolarization, decreased input resistance and inhibited evoked action potentials when applied to cultured dorsal root ganglion neurones. Under whole cell voltage clamp the halitoxins produced an increase in cation conductance that was attenuated by replacing sodium with N-methyl-D-glucamine. Fura-2 fluorescence ratiometric calcium imaging was used to directly measure calcium flux into neurones after exposure to halitoxins. Calcium influx, evoked by the halitoxins, persisted when the neurones were bathed in medium containing the voltage-activated calcium channel antagonists cadmium and nickel. Experiments on undifferentiated F-11 cells showed little or no calcium influx in response to depolarizing concentrations of potassium and indicated that halitoxins evoked massive calcium influx in the absence of voltage-activated calcium channels. The halitoxins also produced transient increases in intracellular calcium when F-11 cells were bathed in calcium-free medium suggesting that the toxins could release calcium from intracellular stores. The pore-forming action of the halitoxins was identified when the toxins were applied to artificial lipid bilayers composed of phosphatidylcholine and cholesterol. Halitoxins evoked channel-like activity in the lipid bilayers, with estimated unitary conductances of between 145pS and 2280pS, possibly indicating that distinct channels could be produced by the different components in the preparation of halitoxins.

Key words: Calcium permeant ion channel — Pore former — Halitoxin — Sensory neurone — Lipid bilayer

Introduction

Recent years have seen the growth of a body of literature relating to a number of secondary metabolites with a common 3-alkyl pyridinium or 3-alkyl piperidine moiety isolated from a variety of genera in the phylum *Porifera* (the sponges) (Andersen, Van Soest & Kong, 1996). Examples of these are the halicyclamines (Jaspars et al., 1994) and the manzamines (Crews et al., 1994). These alkaloids all display marked biological activity and may function as sponge chemical defenses against predation and invasion by microorganisms. Therefore these compounds are of interest for their potential therapeutic properties and as tools for research. Studies aimed at the isolation and characterization of these compounds have elucidated much about their structure and composition. During our work we focused on the structure and electrophysiological properties of one set of these compounds, the 1,3-alkylpyridinium salts (1,3-APS) examples of which are the halitoxins (Fig. 1.1; Schmitz, Hollenbeak & Campbell, 1978) and the amphitoxins (Fig. 1.2; Albrizio et al., 1995). Varied biological activity has been reported for these compounds from cytotoxicity (Schmitz et al., 1978) through to epidermal growth factor inhibition (Davies-Coleman et al., 1993), neurotoxicity (Berlinck et al., 1996) and anticholinesterase activity (Sepcic et al., 1997). The halitoxin compounds have been isolated from a wide number of Haplosclerid genera: *Haliclona erina; Haliclona rubens; Haliclona viridis* (Schmitz et al., 1978); *Amphimedon viridis* (for-

**Present address:* University Chemical Laboratory, Lensfield Road, Cambridge, CB2 1EW

Correspondence to: R.H. Scott

merly *Haliclona viridis*, Berlinck et al., 1996); *Amphimedon compressa* (Albrizio et al., 1995); *Callyspongia fibrosa* (Schmitz et al., 1987) and *Reniera sarai* (Sepcic et al., 1997) suggesting they may have common functional properties as poriferan defense system. 1,3-APS occur as high molecular weight oligomers ranging from 1 KDa to greater than 25 KDa, and it is most likely that they exist as linear oligomers, with varying lengths of aliphatic chains linking the pyridine units. Little is known about the supramolecular structuring of these compounds except for the determination of average hydrodynamic radii of high weight oligomers (Sepcic et al., 1997).

Relatively little work has been carried out on the biological actions of halitoxins, but several previous studies suggest that an electrophysiological investigation would be appropriate. Firstly, Baslow and Turlapaty (1969) identified antitumor activity of halitoxins and at higher doses neurotoxic actions consisting of tremors, convulsions and subsequent paralysis. Secondly, halitoxin has been found to specifically inhibit potassium conductances in frog muscle (Sevcik et al., 1986) and squid axon (Sevcik et al., 1994) preparations. Thirdly, further studies have shown that successive application of halitoxin to a crab nerve preparation depolarizes membrane potential and suppresses action potentials in a dose-dependent manner. Additionally, halitoxin produced dose-dependent lysis of sea urchin eggs. These actions of halitoxins may be indicative of these molecules having nonspecific actions on biological membranes (Berlinck et al., 1996). We have therefore determined the chemical composition of our halitoxin fraction and investigated its actions on cultured DRG neurones, undifferentiated F-11 cells (a mouse dorsal root ganglion neurone × N18TG2 neuroblastoma hybridoma, Platika et al., 1985) and a lipid bilayer preparation.

Materials and Methods

Isolation and Structure Determination

During this study a collection of *Callyspongia ridleyi* from Papua New Guinea was investigated. Collection, solvent extraction and partition were carried out using the standard protocol described earlier (Jaspars et al., 1994). The butanol extract contained the bulk of the 1,3-APS compounds as indicated by nuclear magnetic resonance spectroscopy (NMR). This was applied to a lipophilic Sephadex LH-20 size exclusion column and several fractions were collected. For further investigations we chose the fraction whose molecular weight was shown to be in the range of 5–6 KDa. The molecular weights were determined by matrix-assisted laser desorption ionization time-of-flight mass spectrometry (MALDI-TOF MS).

Calculation of charge distribution in 1-methyl-3-picolinium and 1-methyl pyridinium cations was carried out. This was done in order to gain some insight into the distribution of the +1 charge formally associated with the quaternized nitrogen atom in the 1,3-alkyl pyridinium subunit characteristic of the halitoxins. The model systems 1-methyl-3-picolinium (Fig. 1.4) and 1-methyl pyridinium (Fig. 1.5) were chosen. *Ab-initio* calculations were performed at the MP2/6-31G(d)//RHF/6-31G(d) level using the GAMESS-US quantum-chemical software package (Schmidt et al., 1993) and the partial atomic charges derived from the resulting nuclear geometry and electronic distribution.

Cell Cultures

Primary cultures of DRG neurones were prepared following enzymatic and mechanical dissociation of dorsal root ganglia from decapitated 2-day old Wistar rats. The sensory neurones were plated on laminin-polyornithine coated coverslips and bathed in F14 culture medium (Imperial Laboratories) supplemented with 10% horse serum (Gibco), penicillin (5000 IU/ml), streptomycin (5000 mg/ml), $NaHCO_3$ (14 mM) and nerve growth factor (20 ng/ml). The cultures were maintained for up to 3 weeks at 37°C in humidified air with 5% CO_2, and re-fed with fresh culture medium every 5–7 days.

Undifferentiated F-11 cells from Dr. M.C. Fishman (Massachusetts General Hospital, Boston, MA) were grown as a monolayer on glass coverslips in 30 mm dishes. The cells were bathed in Ham's F-12 culture medium containing 2 mM L-glutamine supplemented with 15% Hyclone fetal bovine serum, HAT supplement (100 μM hypoxanthine/400 nM aminopterin/16 μM thymidine), 100 units/ml penicillin and 100 μg/ml streptomycin. The cultures were maintained at 37°C in humidified air with 5% CO_2, and passed twice a week using mechanical cell dissociation.

Electrophysiology

Experiments were conducted at room temperature (approximately 23°C) on DRG neurones that had been in culture for at least 2 days. The whole-cell recording technique (Hamill et al., 1981) was used to study the actions of halitoxins on membrane potential, evoked action potentials and input resistance. Additionally, under voltage-clamp halitoxin-evoked whole cell currents were investigated. Whole cell recordings were made using either an Axopatch-1D amplifier or an Axoclamp-2A switching voltage-clamp amplifier. Under voltage clamp, seventy to eighty percent series resistance compensation was applied and the Axoclamp-2A was operated at a sampling rate of 15–20 kHz. Low resistance (5–12 MΩ) borosilicate glass patch pipettes were fabricated using a Kopf model 730, needle/pipette puller. The neurones were bathed in a variety of different extracellular solutions. The standard NaCl-based extracellular solution contained in mM: NaCl, 130; KCl, 3.0; $CaCl_2$, 2.0; $MgCl_2$, 0.6; $NaHCO_3$ 1.0, HEPES 10.0, glucose 5.0. The N-methyl-D-glucamine (NMDG)-based extracellular solution contained in mM: NMDG, 166; $CaCl_2$, 2.0; $NaHCO_3$ 1.0, HEPES 10.0, glucose 4.0, tetrodotoxin (TTx, Alomone labs) 0.0025. The NMDG (Ca^{2+}-free)-based extracellular solution contained in mM: NMDG, 166; $NaHCO_3$ 1.0, HEPES 10.0, glucose 4.0, TTx 0.0025. For all the extracellular solutions the pH and osmolarity were adjusted to 7.4 and 310–320 mOsmol/l with NaOH and sucrose, respectively. The patch pipette solution contained in mM: KCl, 140; EGTA, 5; $CaCl_2$, 0.1; $MgCl_2$, 2.0; HEPES, 10.0; ATP, 2.0; and the pH and osmolarity were adjusted to 7.2 with Tris and 310–315 mOsmol/l with sucrose. After entering the whole cell recording configuration, neurones were allowed to equilibrate for 5 min before electrophysiological measurements were made.

For voltage clamp recordings, neurones were held at −90 mV and linear current-voltage relationships were generated with 100 msec voltage step commands to potentials between −170 and −60 mV under control conditions and −170 and +20 mV after halitoxin application.

Halitoxins were applied to the extracellular environment by low pressure ejection via a blunt micropipette (tip diameter about 10 μm) positioned approximately 100 μm from the neurone being recorded. The cells were maintained in a bath and were not continually perfused; drug concentrations declined after pressure ejection as a result of diffusion.

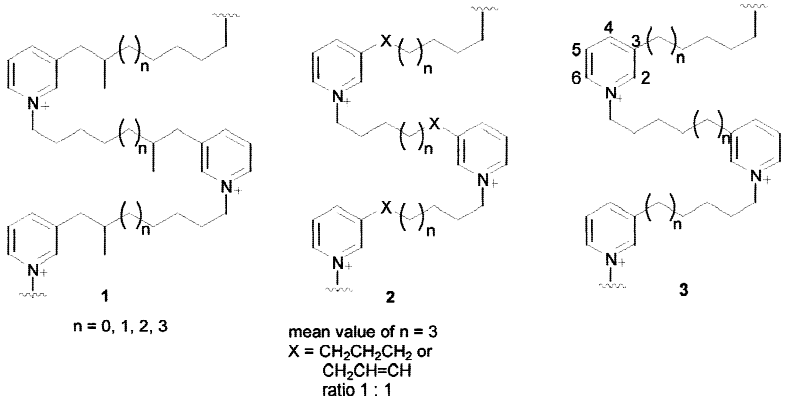

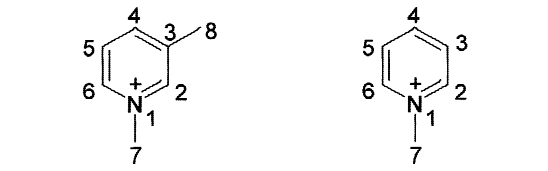

4 5

Fig. 1. Structures of halitoxins and related compounds. (1) halitoxins, (2) amphitoxins and (3) 1,3 alkyl-pyridinium salts with saturated alkyl chains, investigated in this study. Structures of (4) 1-methyl-3-picolinium and (5) 1-methyl pyridinium cations used in the charge distribution calculations.

The electrophysiological data were stored on digital audiotape (DAT) using a DTR-1200 DAT recorder (Biologic) and subsequently analyzed using Cambridge Electronic Design voltage clamp software (version 6). For monitoring changes in membrane potential or holding current continuous records were obtained on a chart recorder (Gould 2200s pen recorder). All data are given as Mean ± SEM and statistical significance was determined, using the Student's two-tailed *t* test, paired or independent where appropriate and *P* values are reported in the text.

Intracellular Calcium Imaging

Cultured DRG neurones and F-11 cells were incubated for 1 hr in NaCl-based extracellular solution containing 10 μM fura-2AM (Sigma, 1 mM stock in dimethylformamide). The cells were then washed for 20 min to remove the extracellular fura-2AM and to allow cytoplasmic de-esterification of the Ca^{2+}-sensitive fluorescent dye. The cells were constantly perfused (1–2 ml/min) and viewed under an inverted Olympus BX50WI microscope with a KAI-1001 S/N 5B7890-4201 Olympus camera attached. The fluorescence ratiometric images from data obtained at excitation wavelengths of 340 nm and 380 nm were viewed and analyzed using OraCal pro, Merlin morphometry temporal mode (Life Sciences resources, version 1.20). All experiments were conducted at room temperature and data are expressed as Means ± SEM.

Lipid Bilayer and Pipette Dipping

The pipette dipping method (Coronado & Latorre, 1983) was used to investigate the actions of halitoxins on artificial planar lipid bilayers. All our recordings were made under voltage-clamp conditions using an Axopatch-1D amplifier and 10 MΩ borosilicate glass patch pipettes dipped in "Sigma-coat" and filled with the KCl-based patch pipette solution. The standard NaCl-based solution was in the bath. Lipid bilayers were formed using a monolayer of phosphatidylcholine (Sigma, type 2s from Soy Bean) and cholesterol (Sigma, grade 1 from Porcine liver), at a molar ratio of 9:1 in HPLC grade *n*-pentane. The tip of the patch pipette was placed in NaCl-based extracellular solution contained in a 35 mm dish and 10 to 30 μl of a 1 mg/ml lipid/*n*-pentane solution was applied to the solution surface. After 2 to 5 min the pentane evaporated from the surface of the monolayer. The patch pipette was gently removed from the solution and then replaced into the solution to form a planar lipid bilayer across the tip of the pipette. The seal resistance of the lipid bilayers ranged from 6 to 32 GΩ. The bilayer seal resistances were stable for 10 to 20 min before halitoxin 50 μg/ml was applied by pressure ejection from a blunt patch pipette.

Results

Chemical Data

By comparison to literature NMR data the structure was identified, *see* Fig. 1.3, with saturated alkyl chains. We were interested in defining the size and size distribution of the alkyl chains in more detail, as it was not clear whether the number *n* in 3 varied within each chain or only between different chains. We used electrospray mass spectrometry (ESI-MS) for this, and the distribution of 1,3-APS monomers is shown in Table 1. It can be seen that there is a preference for 8 and 9 carbon alkyl connecting chains ($n = 4, 5$ in Fig. 1.3), and that a 5 carbon chain is the shortest observed ($n = 1$ in Fig. 1.3).

Analysis of the dimer units from the same ESI mass spectrum indicated that dimers could be formed from various combinations of monomer units (Table 2). The fragmentation process was assumed to be that described

Table 1. Distribution of monomers by ESI-MS in 1,3-APS isolated from *C. ridleyi*

Monomer number	Mass fragment (*m*/*z*)	Monomer unit (inc pyr)	Number of carbons in alkyl chain (value of *n* in Fig. 1.2)	Relative abundance in MS (%)
1	148	$C_{10}H_{14}N^+$	5 (1)	10
2	162	$C_{11}H_{16}N^+$	6 (2)	15
3	176	$C_{12}H_{18}N^+$	7 (3)	13
4	190	$C_{13}H_{20}N^+$	8 (4)	85
5	204	$C_{14}H_{22}N^+$	9 (5)	100
6	218	$C_{15}H_{24}N^+$	10 (6)	36
7	232	$C_{16}H_{26}N^+$	11 (7)	5

Table 2. Dimers observed by ESI-MS and their molecular weights

Monomer	1	2	3	4	5	6	7
1	yes	yes	yes	yes	yes	yes	yes
	295	309	323	337	351	365	379
2		yes	yes	yes	yes	yes	yes
		323	337	351	365	379	393
3			yes	yes	yes	yes	no
			351	365	379	393	
4				yes	yes	no	no
				379	393		
5					no	no	no
6						no	no
7							no

by Davies-Coleman et al., 1993. If each 1,3-APS polymer chain was composed of only one monomer type then we would expect only homodimers to be observed (e.g., 1–1, 2–2, 3–3, etc). However, we see many peaks in the spectrum attributable only to heterodimers (e.g., 1–2, 3–5 etc), suggesting that different monomers are present within each 1,3-APS polymer chain. It is impossible to differentiate between a dimer consisting of say, monomers 2 and 3, and one containing monomers 1 and 4, as these have the same molecular mass, though it is likely that both are present in the mixture. Even segregation into polymers containing only chains with an even or odd number of carbon chains can be ruled out by the existence of such dimers as 1–4 and 2–3 (both *m*/*z* 337). It is interesting to note that no higher molecular weight dimers are present in the mixture, although these are theoretically possible (e.g. 5–5, 6–7, 7–7, etc). The most abundant peaks are at *m*/*z* 379 (48%, 4–4, 3–5, 2–6, 1–7 dimers), 295 (30%, 1–1 dimer) and 393 (28%, 5–4, 3–6, 2–7 dimers), which is in keeping with the observed abundance of the monomers, except for the peak at *m*/*z* 295. We do not know why there is this exceptional peak at *m*/*z* 295, it could be due to the mass spectrometry conditions and 295 being stable to cleavage, but perhaps it relates to the sponge's biochemistry and that the organisms do not produce the monomer at 148.

Besides monomers and dimers only a series of hexamers was observed in the ESI mass spectrum at *m*/*z* 1100–1300. Analysis of isotope patterns showed each of these to contain 5 Cl^- to counterbalance the charge on 6 pyridine N^+. One example is the cluster at *m*/*z* 1185.8 which might be composed of $[(C_{10}H_{14}N)_3 + (C_{11}H_{16}N) + (C_{12}H_{18}N) + (C_{16}H_{26}N)]Cl_5 = C_{69}H_{102}N_6Cl_5$ (MW 1189.7). The system would need to lose four protons which can occur readily in the mass spectrometer during the fragmentation process (Davies-Coleman et al., 1993). A similar analysis can be carried out for the other clusters observed. This again indicates that the 1,3-APS polymer chain is made up of a random sequence of monomers.

The MALDI-TOF MS spectrum showed peaks at *m*/*z* 4713 (38), 4827 (8), 4998 (100), 5510 (8). The base peak at *m*/*z* 4998 translates to roughly 19–27 monomer units (*see* Table 1) in the chain if the chloride ions are included.

NMR Data for the Fraction Which is ~5KDa from Chromatography

δ_H (250 MHz, D_2O, HDO ref. at 4.80 ppm) 8.7 ppm, 2H, s (pyr H2 and pyr H6); 8.4 ppm, 1H, d, $J = 7.3$ Hz (pyr H4); 8.0 ppm, 1H, t, $J = 7.0$ Hz (pyr H5); 4.5 ppm, 2H, t, $J = 7.3$ Hz (N^+-CH_2); 3.2 ppm, 2H, t, $J = 7.6$ Hz (pyr-CH_2); 2.8 ppm, 2H, m (N^+-CH_2-CH_2); 2.0-1.0 ppm, m, (alkyl CH_2). δ_C (62.9 MHz, D_2O) 145 ppm (pyr C4); 144 ppm (pyr C3); 143 ppm (pyr C2); 142 ppm (pyr C6); 128 ppm (pyr C5); 62 ppm (N^+-CH_2); 32 ppm, 31 ppm, 30 ppm, 28 ppm (several peaks), 26 ppm (all alkyl CH_2).

Relative abundance of dimer peaks in ESI-MS (based on *m*/*z* 204 = 100%) 295 (30); 309 (22); 323 (13); 337 (7); 351 (8); 365 (21); 379 (48); 393 (28).

Isotope pattern for cluster beginning at *m*/*z* 1185.8: 1185.8 (50); 1186.9 (33), 1187.8 (100); 1188.7 (63); 1189.8 (70); 1190.8 (50); 1191.9 (33); 1192.8 (17). Calculated for $C_{69}H_{98}N_6Cl_5$: 1185.6 (52); 1186.6 (42); 1187.6 (100); 1188.6 (72); 1189.6 (80); 1190.6 (50); 1191.6 (36); 1192.6 (19). Other hexamer clusters appeared beginning at *m*/*z* 1157.9 (20); 1171.9 (100); 1185.8 (70); 1299.9 (40); 1213.9 (18); 1228.0 (8); 1242.0 (6); 1256.1 (3).

In summary the structures of the compounds studied in this project are given in Fig. 1.3 with *n* ranging from one to seven and the number of monomers ranging from 19 to 27.

Calculation of Charge Distribution in 1-Methyl-3-Picolinium and 1-Methyl Pyridinium Cations

From Table 3 it can be seen that the formal unit positive charge associated with the nitrogen is in fact distributed

over carbons 2 and 6 and all of the protons in the molecule. The nitrogen itself carries a negative charge and would not therefore be expected to interact favorably with anionic species as might be inferred from its formal charge state. As the highest concentration of positive charge occurs on the hydrogens it appears that a less localized electrostatic interaction with the "edge" of the pyridine ring would be more likely.

Comparison with the molecule illustrated in Figs. 1.4 and 5 shows that there is a significant rearrangement of charge on the heavy atoms introduced by the desymmetrization of the aromatic centers. However, the resulting charges on the ring protons are only very slightly effected, as are the charges associated with the nitrogen and its adjacent carbons.

Table 3. Mulliken partial atomic charges obtained from MP2/6-31G(d)//RHF/6-31G(d) calculation on Fig. 1.4 and Fig. 1.5.

	1-Methyl-3-picolinium (4)	1-Methyl pyridinium (5)
ATOM	Charge (units = *e*)	
N1	−0.5849	−0.5863
C2	+0.1350	+0.1607
C3	−0.0493	−0.2698
C4	−0.0943	−0.0869
C5	−0.2738	−0.2721
C6	+0.1599	+0.1652
C7	−0.5182	−0.3340
C8	−0.3331	######
H2	+0.2878	+0.2980
H3	######	+0.2942
H4	+0.2864	+0.2960
H5	+0.2910	+0.2940
H6	+0.2961	+0.2988
H7a*	+0.2389	+0.2404
H7b*	+0.2486	+0.2508
H7c*	+0.2486	+0.2508
H8a*	+0.2099	######
H8b*	+0.2257	######
H8c*	+0.2257	######
TOTAL =	+1.0000	+1.0000

Atomic units used ($1e = 1.602 \times 10^{-19}$ C).

* Note: differences in the charges on methyl protons are due to the fact that one of the three hydrogens in each group lies in the plane of the heavy atoms and hence is subject to a different electrostatic environment than those lying above and below this plane.

Actions of Halitoxins on the Electrophysiological Properties of Cultured DRG Neurones

In this study, three different doses of 0.5, 5.0 and 50 μg/ml halitoxin fraction were used. Given a mean estimated molecular weight of 5 KDa for the toxin preparation the approximate concentrations of halitoxins were 0.1, 1.0 and 10 μM. Under control conditions the resting membrane potential of the cultured DRG neurones was −60 ± 2 mV ($n = 27$). Application of halitoxins for 20 sec caused an apparent dose-dependent depolarization to −26 ± 5 mV ($n = 15$, $P < 0.001$) and −7 ± 1 mV ($n = 9$, $P < 0.001$), for 5 μg/ml and 50 μg/ml halitoxins, respectively. Application of 0.5 μg/ml halitoxins for 20 sec gave no significant change in resting membrane potential. The depolarizations evoked by the halitoxins were associated with significant reductions in the mean input resistances of the DRG neurones. Under control conditions the mean input resistance was 356 ± 42 MΩ ($n = 12$). In the presence of 0.5, 5 and 50 μg/ml halitoxins the mean input resistance values were 283 ± 34 MΩ ($n = 3$, NS), 71 ± 23 MΩ ($n = 6$, $P < 0.05$) and 27 ± 12 MΩ ($n = 3$, $P < 0.02$), respectively. The membrane potential and input resistance did not significantly recover after 20 sec application of the halitoxins, even if the cells were left for 20 min or more (Fig. 2*A*). In a further set of experiments current was injected into the cells to compensate for the depolarizations produced by the halitoxins. This was done so that input resistance and evoked action potentials could be consistently measured from a potential of −70 mV under control conditions and after the halitoxins had been applied. Even when corrections were made for changes in membrane potential significant reductions in input resistance were measured following 20 sec application of 5 and 50 μg/ml halitoxins (Fig. 2*B*). The effects of the halitoxins on input resistance were seen over a wide voltage range (Fig. 2*C*) and were coupled with an inability to activate an action potential even when supramaximal stimuli were applied (Fig. 2*D*). If 5 μg/ml of halitoxins were applied for two periods of about 20 sec then the toxins produced additional changes in membrane potential and input resistance, suggesting that steady-state responses were not achieved using this protocol (Fig. 3*A*). This could be due to the effects of the halitoxins involving a mechanism that could not be saturated, rather than a conventional receptor-ligand interaction. The changes in membrane potential were partially but significantly reversed by perfusion of NMDG-based extracellular solution (Fig. 3*A* and *B*). However, NMDG-based extracellular solution failed to significantly reverse the effects of the halitoxins on input resistance, with mean values of 20 ± 4 MΩ ($n = 3$) and 56 ± 15 MΩ ($n = 4$) in NaCl-based and NMDG-based extracellular solutions, respectively. These results could have been due to the presence of 2.5 μM TTx in the NMDG-based extracellular solution blocking voltage-activated Na^+ channels. To investigate this possibility, responses to halitoxins (50 and 5 μg/ml; n = 3) were evoked in NaCl-based extracellular solution before TTx was applied in an attempt to reverse part of the toxins actions. Application of TTx (2.5 μM) did not cause any change in either the membrane potential or input resistance after treatment with halitoxins (Fig. 3*C*), which

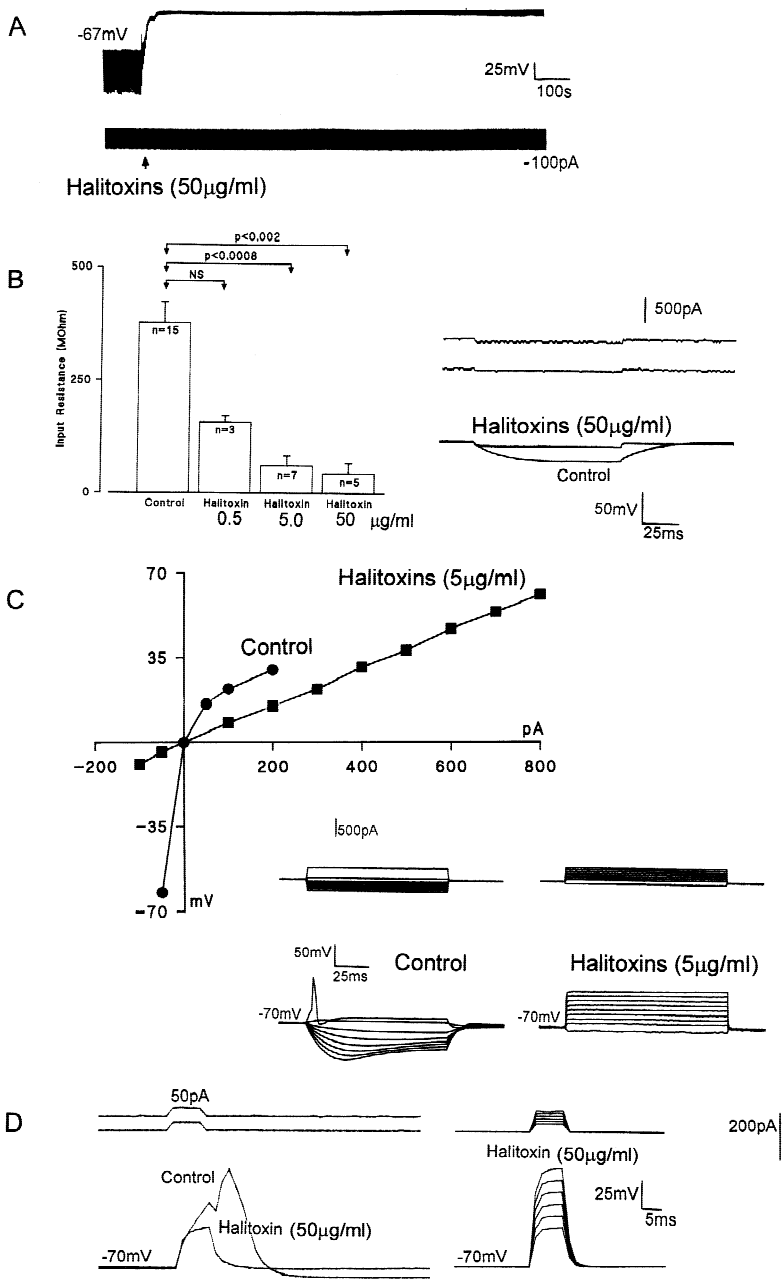

Fig. 2. Electrophysiological actions of halitoxins on cultured DRG neurones. (*A*) Record showing depolarization and change in input resistance produced by a 20 sec application of halitoxins (50 μg/ml). Electrotonic potentials were evoked by −100 pA hyperpolarizing current commands of 100 msec durations applied every 3 sec. (*B*) Bar chart showing the mean input resistances of neurones under control conditions and after exposure to varying concentrations of halitoxins. All measurements were made from a clamp potential of −70 mV. The inset traces show current commands and electrotonic potentials recorded in the absence (Control) and presence of halitoxins. (*C*) Current/voltage relationships obtained under control conditions (filled circles) and after 20 sec application of halitoxins (filled squares). Inset records show example current commands and potentials recorded from a clamp potential of −70 mV, under control conditions and after application of halitoxins. (*D*) Records show the abolition of an evoked action potential (control) by halitoxins. The right hand records show that this effect could not be overcome by supramaximal depolarizing current commands.

suggests that the effect of NMDG-based extracellular solution was due to lower permeability of the large cation compared with Na^+.

Under voltage-clamp conditions 50 μg/ml of halitoxins produced such large inward currents it was not possible to clamp the neurones and so further studies were carried out with 5 μg/ml. The neurones were voltage clamped at −90 mV and current/voltage relationships generated under control conditions and after application of the toxins. Under control conditions neurones were not depolarized to potentials positive to −60 mV, because the linear, (ohmic) current-voltage relationship would be contaminated with voltage-activated conductances. This was not a problem after application of the halitoxins that evoked large inward currents with a mean value of −2.65 ± 0.51 nA ($n = 5$) from a holding potential of −90 mV, and appeared to abolish voltage-activated currents. In NaCl-based extracellular medium the mean conductance and reversal potential for the current evoked by halitoxins were 30 ± 6 μS and −1 ± 4 mV, respectively ($n = 5$, Fig. 4*A*). In NMDG-based extracellular solution (with Ca^{2+} present), the current evoked by halitoxins had a reduced conductance of 12 ± 4 μS ($n = 5$, $P < 0.02$) and a more hyperpolarized reversal potential of −40 ± 9 mV

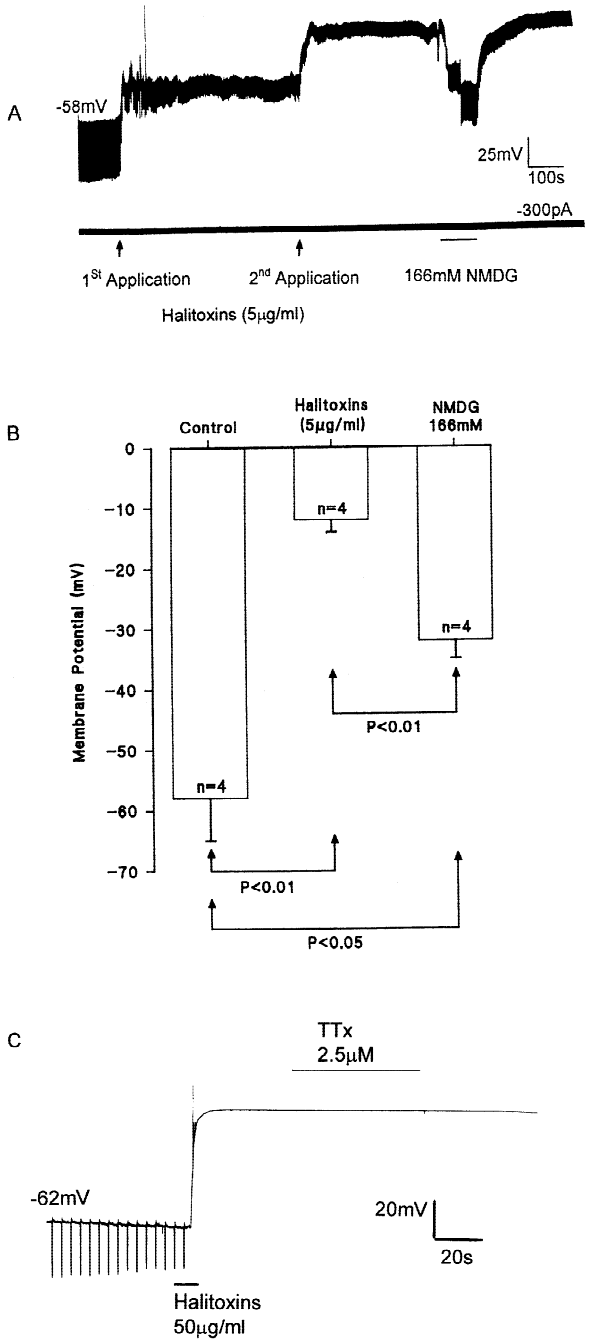

Fig. 3. NMDG-based recording medium attenuated the effects of halitoxins on membrane potential. (*A*) A recording, showing the effects of two applications of halitoxins on membrane potential and input resistance. Electrotonic potentials were evoked every 3 sec by 100 sec hyperpolarizing current commands (−300 pA). Application of NMDG-based extracellular solution caused a partial repolarization of membrane potential. (*B*) Bar chart showing the mean membrane potentials for four neurones under control conditions, after application of halitoxins in NaCl-based extracellular solution and after the response to the halitoxins but during application of NMDG-based extracellular solution. (*C*) A recording showing that 2.5 μM TTx in NaCl-based extracellular solution failed to reverse the actions of halitoxins on membrane potential and input resistance.

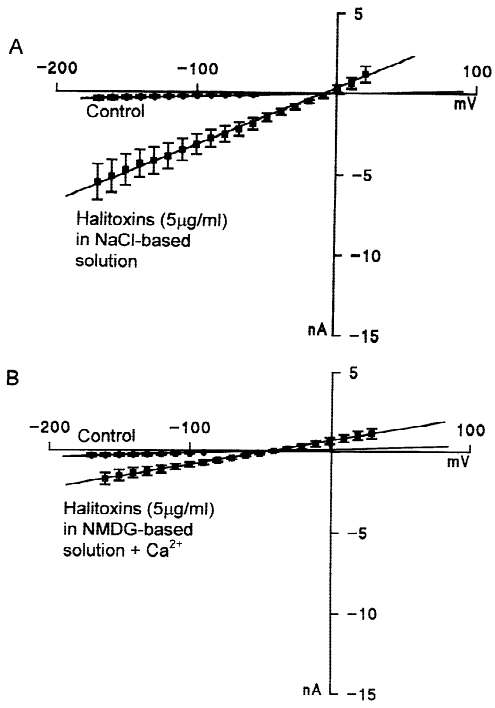

Fig. 4. Current/voltage relationships under voltage clamp in the presence of NaCl-based extracellular solution (*A*) and in the presence of NMDG-based extracellular solution (*B*). In both cases the neurones were voltage-clamped at a holding potential of −90 mV. Depolarizing and hyperpolarizing voltage step commands were applied for 100 msec to generate current-voltage relationships before (Control) and after application of halitoxins. Mean data ± SEM are presented, and $n = 5$ for each experiment.

($n = 5$, $P < 0.05$, Fig. 4*B*). These results suggested significant components of the conductances were due to Ca^{2+} and/or NMDG. Experiments carried out in NMDG-Ca^{2+} free extracellular solution gave anomalous results. No significant difference for the conductance of the halitoxins-evoked current was seen but a significant depolarizing shift in the reversal potential to -20 ± 2 mV ($n = 4$), compared with the data obtained with NMDG-based solution containing 2 mM Ca^{2+} was recorded. This result suggested that the current evoked by the halitoxins involved both Ca^{2+} and NMDG influx, but that Ca^{2+} may antagonize or produce charge-screening effects to influence the flux of NMDG, analogues to mole fraction phenomena. To investigate the influx of Ca^{2+} we subsequently used fura-2 loaded DRG neurones and imaging techniques.

Investigation of Calcium Influx Evoked in DRG Neurones by Halitoxins

In this part of the study we distinguished between cultured DRG neurones and background cells such as glia and fibroblasts in the primary culture by the rise in in-

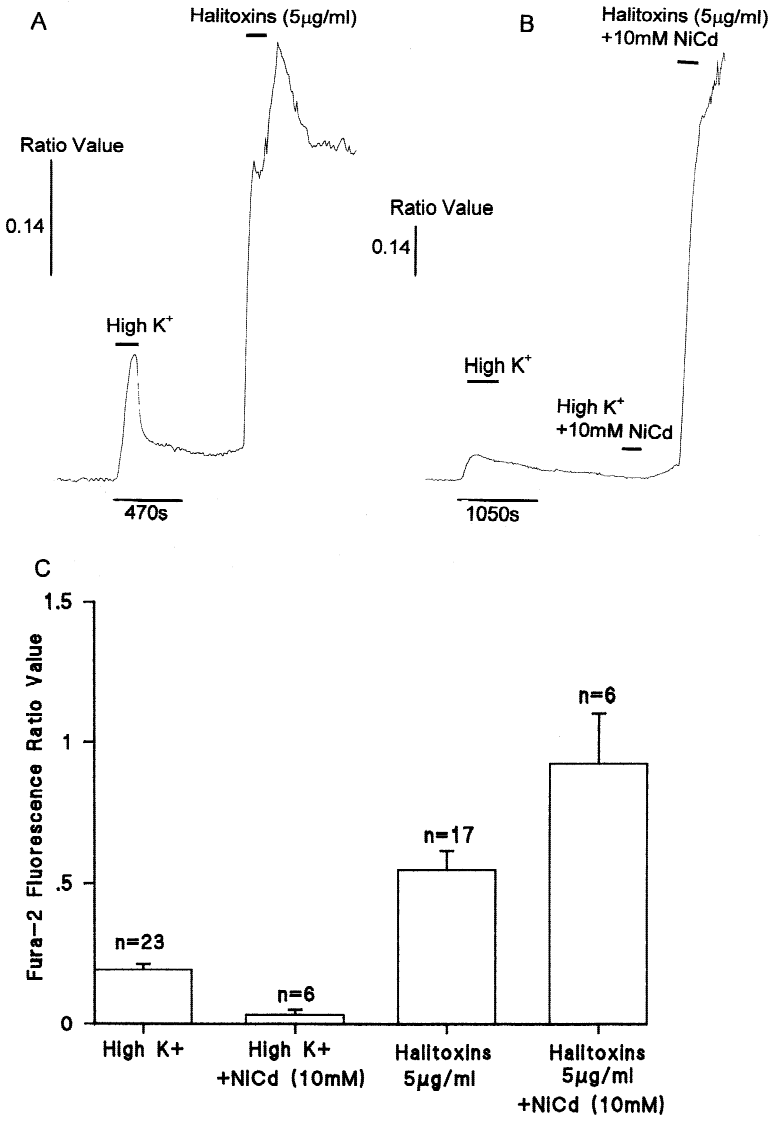

Fig. 5. Halitoxins evoked increases in intracellular Ca^{2+} in cultured DRG neurones. Increases in intracellular Ca^{2+} were detected as changes in the fluorescence ratio values using neurones loaded with the Ca^{2+}-sensitive dye, fura-2. (*A*) Mean ($n = 16$) plot for fluorescence ratio indicating increases in intracellular Ca^{2+} evoked by perfusion of NaCl-based extracellular solution containing high K^+ and halitoxins. (*B*) Mean ($n = 6$) plot for fluorescence ratio indicating increases in intracellular Ca^{2+} evoked by perfusion of NaCl-based extracellular solution containing high K^+ but no response when 10 mM $NiCl_2$ and $CdCl_2$ were simultaneously applied with high K^+. The halitoxins continued to evoke increases intracellular Ca^{2+} when they were applied simultaneously with the voltage-activated Ca^{2+} channel blockers $NiCl_2$ and $CdCl_2$. (*C*) Bar chart, showing the mean changes in fluorescence ratio values observed in response to high K^+ and halitoxins applied in the absence and presence of 10 mM $NiCl_2$ and $CdCl_2$ (NiCd).

traneuronal Ca^{2+} observed in response to high (30 mM) extracellular K^+-evoked depolarization and thus activation of voltage-gated Ca^{2+} channels. In our cultures the non-neuronal background cells load with fura-2 but do not express voltage-gated Ca^{2+} channels and thus do not show a rise in intracellular Ca^{2+} when perfused with high K^+ extracellular solution. Halitoxins (5 μg/ml) evoked substantial rises in intracellular Ca^{2+} as reflected by increases in the fura-2 fluorescence ratio values both in cultured DRG neurones (Fig. 5*A*) and in non-neuronal cells. Extracellular solution containing the voltage-gated Ca^{2+} channel inhibitors Ni^{2+} and Cd^{2+} (100 μM) failed to attenuate the K^+-evoked rise in intraneuronal Ca^{2+}. The mean values for the increases in fluorescence ratio induced by high K^+ were 0.19 ± 0.02 ($n = 23$) and 0.19 ± 0.03 ($n = 19$) under control conditions and in the presence of 100 μM Ni^{2+} and Cd^{2+}, respectively. The nature of the stimulus (high K^+) required higher concentrations of the Ca^{2+} channel inhibitors to block responses. At 10 mM Ni^{2+} and Cd^{2+} reduced the increase in fluorescence ratio produced by high K^+ to 0.03 ± 0.02 ($n = 6$), but failed to significantly attenuate the rise in intracellular Ca^{2+}-evoked by the halitoxins (Fig. 5*B* and *C*).

Investigation of Calcium Influx Evoked in F-11 Cells by Halitoxins

Undifferentiated F-11 cells were then used to further investigate the rise in intracellular Ca^{2+}-evoked by the halitoxins. In an undifferentiated state these F-11 cells were thought not to express voltage-gated Ca^{2+} channels. However, the undifferentiated F-11 cells were not a homogeneous population of cells and small but detectable

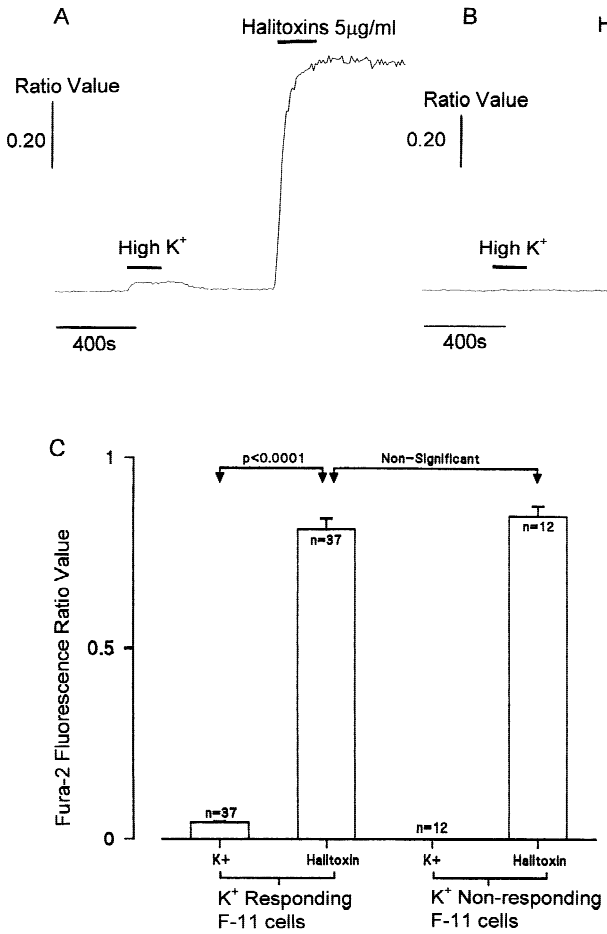

Fig. 6. Halitoxins evoked increases in intracellular Ca^{2+} in F-11 cells. (*A*) Record shows an example from an F-11 cell that showed a modest but detectable change in intracellular Ca^{2+} in response to high K^+-evoked depolarization. Subsequent application of halitoxins evoked a significantly larger rise in intracellular Ca^{2+}. (*B*) Record from an F-11 cell which did not respond to high K^+ but halitoxins still evoked a large increase in intracellular Ca^{2+}. (*C*) Bar chart, showing the mean responses to halitoxins in F-11 cells which responded to high K^+ and F-11 cells which did not respond to high K^+.

changes in intracellular Ca^{2+} in response to high K^+ were measured in 37 out of 49 cells (Fig. 6*A*). The responses to high K^+ obtained from F-11 cells were significantly smaller compared to those seen in cultured DRG neurones ($P < 0.0001$). As was seen with the primary cultures both populations of F-11 cells responded similarly to the halitoxins (5 μg/ml) with massive rises in intracellular Ca^{2+} (Fig. 6*A–C*).

Experiments were conducted to examine whether the halitoxins influenced intracellular Ca^{2+} by causing release of Ca^{2+} from intracellular stores. Surprisingly, in extracellular Ca^{2+}-free conditions (with 2.5 mM EGTA and no added $CaCl_2$) halitoxins (5 μg/ml)-evoked large transient increases in intracellular Ca^{2+} (mean change in fluorescence ratio value of 0.78 ± 0.06, $n = 21$; Fig. 7*A*). These transient Ca^{2+} responses persisted when extracellular Na^+ was replaced by NMDG to reduce the ionic disturbance produced by the halitoxins (mean change in fluorescence ratio value of 0.57 ± 0.06, $n = 13$; Fig. 7*B*). When the F-11 cells were subsequently exposed to extracellular Ca^{2+} again changes in intracellular Ca^{2+} were detected (Fig. 7*A* and *B*). This indicated that the transient nature of the responses to halitoxins observed in Ca^{2+}-free conditions was not due to a loss of fura-2 from the cells. These observations suggest that the halitoxins released Ca^{2+} from intracellular stores of F-11 cells. Experiments were then conducted with 140 mM KCl but no Ca^{2+} in the extracellular solution. Under these conditions little ionic disturbance is likely yet halitoxins evoked transient increases in intracellular Ca^{2+} with a mean change in fluorescence ratio value of 0.37 ± 0.04 ($n = 13$ out of 31 cells). However, it was clear that 18 cells did not respond to halitoxins under these conditions. Changing from the standard NaCl-based extracellular recording solution to KCl-based, Ca^{2+}-free solution evoked transient changes in intracellular Ca^{2+} in 18 out of 31 cells. Under these conditions the mean change in fluorescence ratio value was 0.24 ± 0.04 ($n = 18$). The cells that responded to perfusion with KCl-based, Ca^{2+}-free solution did not subsequently respond to halitoxins (Fig. 7*C*). One interpretation of these observations is that the KCl-based, Ca^{2+}-free solution caused depletion of intracellular Ca^{2+} stores and that these stores could not be refilled when the cells were bathed with Ca^{2+}-free extracellular solution. Hence, when the intracellular Ca^{2+} stores were depleted the halitoxins could not mo-

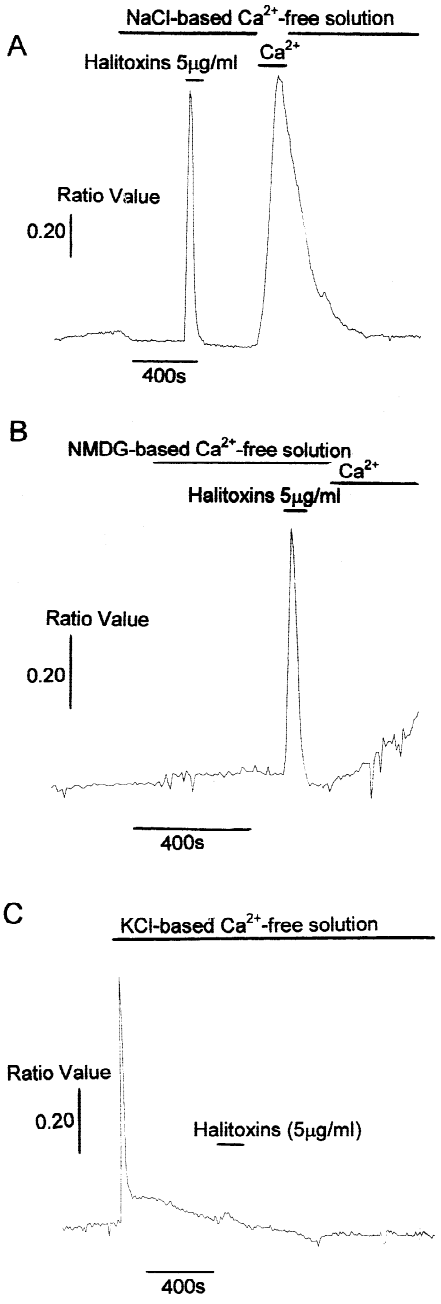

Fig. 7. Halitoxins evoked transient rises in intracellular Ca^{2+} when applied in Ca^{2+}-free extracellular solutions. (*A*) Record from an F-11 cell bathed in NaCl-based Ca^{2+}-free solution. Halitoxins evoked transient rises in intracellular Ca^{2+} and a further response was observed when NaCl-based extracellular solution containing 2 mM Ca^{2+} was perfused. (*B*) Record from an F-11 cell bathed in NMDG-based Ca^{2+}-free solution. Halitoxins evoked transient rises in intracellular Ca^{2+} and a further slow response was observed when NMDG-based extracellular solution containing 2 mM Ca^{2+} was perfused. (*C*) Example record, showing the response in an F-11 to perfusion with KCl-based, Ca^{2+}-free solution and no subsequent response to halitoxins. In all these experiments the cells were loaded with fura-2 and initially perfused with standard NaCl-based extracellular solution.

bilize intracellular Ca^{2+}. It was also noted that cells exposed to KCl-based, Ca^{2+}-free solution did not respond to 10 mM caffeine.

Pore Forming Effects of Halitoxins on Artificial Lipid Bilayers

The lack of specificity and large sizes of conductance changes observed in response to the halitoxins in this study and previous findings suggested that the 1,3 alkyl-pyridinium salts may act as pore formers rather than activators of native channels. This was investigated directly by applying the halitoxins (50 μg/ml) to artificial lipid bilayers (composed of 9:1, phosphatidylcholine and cholesterol) formed across the tip of patch pipettes. Application of the toxins, after a delay of approximately 50 sec, caused the development of a range of unitary channel-like events in lipid bilayers which had previously been "silent," or stable (Fig. 8*A*). After a variable period these events summated to give a macrocurrent. Unitary current amplitudes were measured at transmembrane potentials of −90 and +90 mV and with the estimated current reversal potential were combined to give estimates of the unitary conductances. The estimated current reversal potential was determined from the difference currents. Prior to application of halitoxins and after activation by the toxins of a stable macrocurrent, current/voltage relationships were generated between −180 mV and 0 mV, using 100 msec voltage-step commands. The control current-voltage relationship was subtracted from the relationship obtained after evoking a current with halitoxins and reversal potential of the resulting difference current was measured. The main difficulty encountered was the great variability within a single lipid bilayer between the amplitudes of the channel-like events. At −90 mV the amplitudes of the currents varied between −10 pA and −175 pA. Similarly, at +90 mV the current amplitudes varied between +15 pA and +144 pA ($n = 2$ bilayers). The estimates for the unitary conductances caused by the halitoxins were 145 pS to an upper limit of 2280 pS (Fig. 8*B* and *C*).

Discussion

Halitoxins (1,3 alkyl-pyridinium salts) produced dramatic effects on the electrophysiological properties of cultured DRG neurones, F-11 cells and artificial lipid bilayers. The actions of these toxins included irreversible depolarizations, large increases in input conductance, loss of measurable action potentials and loss of measurable voltage-activated currents. These effects are consistent with halitoxins producing ion permeable channels in cell membranes and thus large increases in input conductance on top of which it is not possible to detect

native conductances. Our results are also consistent with those from previous work showing a decline in action potential amplitude (Berlinck et al., 1996) and block of squid axon K^+ conductances (Sevcik et al., 1994) by sponge toxins. The halitoxin pores appeared to have a high permeability to divalent Ca^{2+} and the large organic monovalent cation $NMDG^+$. The Ca^{2+} permeability might have been due to depolarization-induced activation of voltage-gated Ca^{2+} channels. However, the responses to halitoxins were significantly greater than those produced by high K^+-evoked depolarizations. Additionally, the measurements from nonneuronal cells in primary cultures, DRG neurones bathed in high concentrations of Cd^{2+} and Ni^{2+} and F-11 cells which did not respond to high K^+ suggest that functional voltage-activated Ca^{2+} channels were not required for the halitoxins to produce massive influx of Ca^{2+} into cells. The Ca^{2+} component of the conductance evoked by halitoxins observed in this study also provides a potential mechanism by which toxins from *Haliclona viridis* induced concentration and Ca^{2+}-dependent release of gamma-aminobutyric acid from rat olfactory bulb neurones (Jaffe, Eisig & Sevcik, 1993).

Surprisingly, halitoxins also evoked release of Ca^{2+} from intracellular stores. This was revealed under extracellular Ca^{2+}-free conditions and may involve loss of Ca^{2+} from a variety of organelles including endoplasmic reticulum and mitochondria. The data from experiments using a high K^+ and Ca^{2+}-free extracellular solution suggested that if intracellular stores were depleted of Ca^{2+} then halitoxins failed to produce transient increases in intracellular Ca^{2+}. Several possible mechanisms may account for this effect of halitoxins on intracellular Ca^{2+} stores. Firstly, the intracellular ionic disturbance produced by the pore-forming toxins may have triggered release of Ca^{2+} from intracellular stores. However, the results obtained with NMDG- and KCl-based extracellular solutions containing no Ca^{2+} make this possibility less likely. Secondly, the organelles containing Ca^{2+} may be in very close proximity to the cell membrane so that the pore formers in spanning the cell membrane gain access to the intracellular store membranes. Release of Ca^{2+} from a store may subsequently result in Ca^{2+}-induced Ca^{2+} release and thus the substantial global responses observed. The third possibility stems from the variable size of the halitoxin molecules and that large pores formed by the larger toxin molecules may provide pathways by which smaller toxin molecules gain access to the intracellular environment and then subsequently produce channels in the intracellular Ca^{2+} stores. Previously it has been shown that serum-derived complement causes insertion of damaging membrane attack complex and increases in intracellular Ca^{2+} in oligodendroglia. This effect of serum-derived complement is dependent on the terminal complement component C9. Interestingly, intracellular Ca^{2+} oscillations in oligodendroglia are also evoked by a 26 amino acid peptide called melittin which has regions of complete homology with the C9 amino acid sequence (Wood et al., 1993). This effect may be indicative of an effect on endoplasmic reticular Ca^{2+} stores by these agents that potentially produce pore-forming lesions. Additionally, it has recently been shown that the transmembrane pore former, perforin, produces disruption of endosomal trafficking. This effect indicates that this pore former also influences the functional properties of intracellular organelles (Browne et al., 1999).

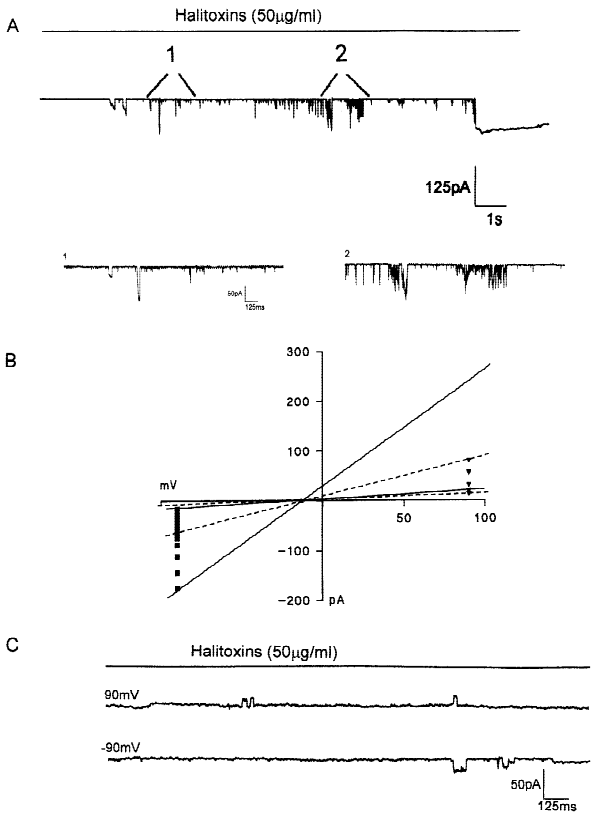

Fig. 8. Halitoxins act as pore formers on artificial lipid bilayers. (*A*) Record of channel-like activity evoked when halitoxins were applied to a lipid bilayer. The lipid bilayer was stable with no channel-like activity for 20 min before application of the halitoxins; 1 and 2 show regions of interest that have been expanded below. (*B*) Unitary current-voltage relationships from a single lipid bilayer experiment. The graph shows the great variation in channel current amplitude at −90 and +90 mV. The lines are the range of predicted slope conductances from currents measured at −90 mV (filled lines) and from currents measured at +90 mV (broken lines). (*C*) Single channel-like events produced by halitoxins when the transmembrane potential was at + 90 and −90 mV.

Direct evidence for the pore-forming properties of the halitoxins investigated in this study came from work on artificial lipid bilayers. Very varied and large unitary conductances were obtained for halitoxin channels. Some of these unitary conductance values are above the

upper theoretical limit (~300 pS) for typical native channels activated by neurotransmitters or voltage (Hille, 1992). However, large conductance channels have been reported for a number of pore-forming toxins, antibiotics and detergents. For example, α-toxin of *Staphylococcus aureus* forms two main classes of channel with conductances of 90 pS and 450 pS in 0.5 M KCl (Menestrina, 1986; Mellor, Thomas & Sansom, 1988) and an estimated pore diameter of 2–3 nm (Fussle et al., 1981; Bayley, 1997). Hemolysin from *Escherichia coli* produces channels with conductances of 500 pS in 0.15 M KCl and a pore diameter of about 1 nm (Benz et al., 1989). Ducloheir and colleagues (1998) found that antiamoebin, the fungal polypeptide antibiotic, forms pores with a range of single channel conductances (90, 480, 960, 1600 & 3200 pS, in 1 M KCl). Similarly, δ-endotoxins form channels with conductances ranging from 200 pS to about 4000 pS in 300 mM KCl (Slatin, Abrams & English, 1990). Large channels with a minimium pore diameter of 9 Å such as those formed by colicin E1 are also permeable to organic monovalent cations such as $NMDG^+$ which have dimensions of 13.3 × 5.5 Å (Bullock, Kolen & Shear, 1992). So the NMDG permeability and large conductance of the channels formed by the halitoxins is on a par with some other pore-forming agents. The variability of the channels formed may be due to the different sized 1,3 alkyl-pyridinium salts present in the preparation of halitoxins. It is not at present possible to separate out the distinct 1,3 alkyl-pyridinium salts, however they are amenable to chemical synthesis and this in the future will be an approach used to investigate the properties of the different halitoxin molecules. Further properties of these 1,3 alkyl-pyridinium salts which makes them attractive for further studies is their high water solubility and chemical stability.

From all of our experiments we predict that the halitoxin channel-like activity shows a degree of cation selectivity with K^+ and Na^+ permeabilities being similar. The permeability to Ca^{2+} appears very significant but less than for K^+ and Na^+. The large cation, $NMDG^+$ has the lowest permeability of the cations studied, never the less $NMDG^+$ conductance is clear following application of halitoxins. Detailed analysis of permeability sequences for a wide range of cations and anions is yet to be undertaken but will benefit from the preparation and use of a single and chemically defined halitoxin compound. In one important respect it is perhaps surprising that halitoxins generate cation-conducting pores given that the formal depiction of the molecules indicates polymers with strong positive charge. However, electronic calculations predict that the charge is delocalized with a small negative charge on the nitrogens of the pyridinium rings that were formally positive. Once complexed to the lipid membrane halitoxins may be nearly electrically neutral, rather than strongly positively charged. An additional consideration in the context of halitoxins forming cation permeable pores may be the interaction with counter anions and specifically Cl^- in physiological solutions and sea water.

The pore-forming effects of the halitoxin preparation was observed with quite low and biologically relevant concentrations. After partial purification, halitoxins make up at least 0.05% of the dry weight of the organism, which suggests the toxins are produced by sponges in great amounts. This could pose sponges with a particular difficulty of pore-forming toxin storage, unless the chemical defense was produced on demand. It seems likely that the halitoxins are produced in the copious enzyme-rich slime secreted by the colony after injury.

Conclusions

Our results suggest that halitoxins insert into biological and artificial lipid membranes to form ion permeable pores that allow flux of monovalent cations including the large organic ion NMDG and the divalent cation Ca^{2+}. A number of potential applications for stable pore formers are apparent (Bayley, 1997). These applications include, use as electrophysiological tools, development of novel cytotoxic molecules and possibly agents for intracellular drug delivery. The synthesis of numerous diverse and stable pore formers with distinct biophysical properties is an exciting future prospect that may be realized through the manipulation of 1,3 alkyl-pyridinium salts.

The butanolic extract of *Callyspongia ridleyi* was a generous gift from Professor Phil Crews, University of California, Santa Cruz. MALDI-TOF MS were carried out by Ian Davidson at the Proteome Unit, Institute of Medical Sciences, Aberdeen University. ESI-MS was carried out by Gary Duncan at the Rowett Research Institute, Aberdeen. RHS thanks The Wellcome Trust and Pfizer UK for support and Dr. Ian Duce for helpful discussion.

References

Albrizio, S., Ciminiello, P., Fattorusso, E., Magno, S., Pawlik, J.R. 1995. Amphitoxin, a new high molecular weight anti-feedant pyridinium salt from the Caribbean sponge *Amphimedon compressa. J. Nat. Prod.* **58:**647–652

Andersen, R.J., van Soest, R.W.M., Kong, F. 1996. *In:* Alkaloids: Chemical and Biological Perspectives. S.W. Pelletier, Editor. Vol. 10: pp. 430. Pergamon, Oxford

Baslow, M.H., Turlapaty, P. 1969. In vivo antitumor activity and other pharmacological properties of halitoxin obtained from the sponge *Haliclona viridis. Proc. West Pharmacol. Soc.* **12:**6–8

Bayley, H. 1997. Building doors into cells. *Sci. Am.* **277:**62–67

Benz, R., Schmid, A., Wagner, W., Goebel, W. 1989. Pore formation by the *Escherichia coli* hemolysin: evidence for an association-dissociation equilibrium of the pore-forming aggregates. *Infect. Immun.* **57:**887–895

Berlinck, R.G., Ogawa, C.A., Almeida, A.M., Sanchez, M.A., Malpezzi, E.L., Costa, L.V., Hajdu, E., de Freitas, J.C. 1996. Chemical and pharmacological characterization of halitoxin from *Amphimedon viridis* (Porifera) from the southeastern Brazilian coast. *Comp. Biochem. Physiol.* **115C:**155–163

Browne, K.A., Blink, E., Sutton, V.R., Froelich, C.J., Jans, D.A., Trapani, J.A. 1999. Cytosolic delivery of granzyme B by bacterial toxins: evidence that endosomal disruption, in addition to transmembrane pore formation, is an important function of perforin. *Mol. Cell Biol.* **19:**8604–8615

Bullock, J.O., Kolen, E.R., Shear, J.L. 1992. Ion selectivity of colicin E1: II. Permeability of organic cations. *J. Membrane Biol.* **128:** 1–16

Coronado, R., Latorre, R. 1983. Phospholipid bilayers made from monolayers on patch-clamp pipettes. *Biophys. J.* **43:**231–236

Crews, P., Cheng, X.C., Adamczeski, M., Rodriguez, J., Jaspars, M., Schmitz, F.J., Traeger, S.C., Pordesimo, E.O. 1994. 1,2,3,4-Tetrahydro-2-N-Methyl-8-Hydroxymanzamine A: an Alkaloid Salt from the Sponge *Petrosia contignata*. *Tetrahedron* **50:**13567–13574

Davies-Coleman, M.T., Faulkner, D.J., Dubowchik, G.M., Roth, G.P., Polson, C., Fairchild, C. 1993. A new EGF-active polymeric pyridinium alkaloid from the sponge *Callyspongia fibrosa. J. Org. Chem.* **58:**5925–5930

Duclohier, H., Snook, C.F., Wallace, B.A. 1998. Antiamoebin can function as a carrier or as a pore-forming peptaibol. *Biochim. Biophys. Acta* **1415:**255–260

Fussle, R., Bhakdi, S., Sziegoleit, A., Tranum-Jensen, J., Kranz, T., Wellensiek, H.J. 1981. On the mechanism of membrane damage by *Staphylococcus aureus* alpha-toxin. *J. Cell Biol.* **91:**83–94

Hamill, O.P., Marty, A., Neher, E., Sakmann, B., Sigworth, F. 1981. An improved patch clamp technique for high resolution current recordings from cells and cell free membrane patches. *Pfluegers Arch.* **391:**85–100

Hille, B. 1992. Ionic Channels of Excitable Membranes. 2nd Edition, pp. 332. Sinauer Associates, Sunderland, MA

Jaffe, E., Eisig, M., Sevcik, C. 1993. Effect of a toxin isolated from the sponge *Haliclona viridis* on the release of gamma-aminobutyric acid from rat olfactory bulb. *Toxicon* **31:**385–396

Jaspars, M., Pasupathy, V., Crews, P. 1994. A tetracyclic diamine alkaloid, halicyclamine A, isolated from the marine sponge *Haliclona sp. J. Org. Chem.* **59:**3253–3255

Jaspars, M., Rali, T., Laney, M., Schatzman, R.C., Diaz, M.C., Schmitz, F.J., Pordesimo, E.O., Crews, P. 1994. The search for inosine 5′ dehydrogenase (IMPDH) inhibitors from marine sponges. Evaluation of the bastadin alkaloids. *Tetrahedron* **50:**7367–7374

Mellor, I.R., Thomas, D.H., Sansom, M.S. 1988. Properties of ion channels formed by *Staphylococcus aureus* delta-toxin. *Biochim. Biophys. Acta* **942:**280–294

Menestrina, G. 1986. Ionic channels formed by *Staphylococcus aureus* alpha-toxin: voltage-dependent inhibition by divalent and trivalent cations. *J. Membrane Biol.* **90:**177–190

Platika, D., Boulos, M.H., Baizer, L., Fishman, M.C. 1985. Neuronal traits of clonal cell lines derived by fusion of dorsal root ganglia neurons with neuroblastoma cells. *Proc. Natl. Acad. Sci. U.S.A.* **82:**3499–3503

Schmidt, M.W., Baldridge, K.K., Boatz, J.A., Elbert, S.T., Gordon, M.S., Jensen, J.J., Koseki, S., Matsunaga, N., Nguyen, K.A., Su, S., Windus, T.L., Dupuis, M., Montgomery, J.A. 1993. General atomic and molecular electronic-structure system. *J. Comput. Chem.* **14:**1347–1363

Schmitz, F.J., Hollenbeak, H.H., Campbell, D.C. 1978. Marine natural products: halitoxin, toxic complex of several marine sponges of the genus *Haliclona. J. Org. Chem.* **43:**3916–3922

Sepcic, K., Guella, G., Mancini, I., Pietra, F., Dalla Serra, M., Menestrina, G., Tubbs, K., Macek, P., Turk, T. 1997. Characterization of anticholinesterase-active 3-alkylpyridinium polymers from the marine sponge *Reniera sarai* in aqueous solutions. *J. Nat. Prod.* **60:**991–996

Sevcik, C., Alvarez-Vasquez, F., Saavedra, J.A., Cordovez, G. 1986. Blockage of resting potassium conductance in frog muscle fibers by a toxin isolated from the sponge *Haliclona viridis. Toxicon* **24:**851–860

Sevcik, C., Garcia-Rodriguez, A.I., D'Suze, G., Mijares, A.J. 1994. Specific blockage of squid axon resting potassium permeability by *Haliclona viridis* (*Porifera: Haliclonidae*) toxin (HvTX). *Toxicon* **32:**773–788

Slatin, S.L., Abrams, C.K., English, L. 1990. Delta-endotoxins form cation-selective channels in planar lipid bilayers. *Biochem. Biophys. Res. Commun.* **169:**765–772

Wood, A., Wing, M.G., Benham, C.D., Compston, D.A. 1993. Specific induction of intracellular calcium oscillations by complement membrane attack on oligodendroglia. *J. Neurosci.* **13:**3319–3332